

Quantum phase transition in the heavy-fermion compound YbIr_2Si_2

H. Q. Yuan,^{1,2,*} M. Nicklas,¹ Z. Hossain,^{1,3} C. Geibel,¹ and F. Steglich¹

¹Max Planck Institute for Chemical Physics of Solids, Nöthnitzer Straße 40, 01187 Dresden, Germany

²Department of Physics, University of Illinois at Urbana-Champaign, 1110 West Green Street, Urbana, Illinois 61801, USA

³Department of Physics, Indian Institute of Technology, Kanpur-208016, India

(Received 1 July 2006; revised manuscript received 6 October 2006; published 15 December 2006)

We investigate the pressure-temperature phase diagram of YbIr_2Si_2 by measuring the electrical resistivity $\rho(T)$. In contrast to the widely investigated YbRh_2Si_2 , YbIr_2Si_2 is a paramagnetic metal below $p_c \approx 8$ GPa. Interestingly, a first-order, presumably ferromagnetic, transition develops at p_c . Similar magnetic properties were also observed in YbRh_2Si_2 and YbCu_2Si_2 at sufficiently high pressures, suggesting a uniform picture for these Yb compounds. The ground state of YbIr_2Si_2 under pressure can be described by Landau Fermi-liquid theory, in agreement with the nearly ferromagnetic Fermi-liquid model. Moreover, evidence of a weak valence transition, characterized by a jump of the Kadowaki-Woods ratio as well as an enhancement of the residual resistivity ρ_0 and of the quasiparticle-quasiparticle scattering cross section, is observed around 6 GPa.

DOI: 10.1103/PhysRevB.74.212403

PACS number(s): 75.20.En, 71.27.+a, 71.10.Hf, 73.43.Nq

The study of quantum critical phenomena has attracted considerable attention because of the fascinating physical properties caused by quantum fluctuations. In the Ce-based heavy fermion (HF) systems, unconventional superconductivity, most likely paired via antiferromagnetic (AFM) spin fluctuations, has been widely observed around a spin-density-wave (SDW) type quantum critical point (QCP).¹ On the other hand, YbRh_2Si_2 has been established as a model system to study quantum physics at a “local” QCP,² around which no superconductivity has yet been observed at $T > 10$ mK. Recent efforts have been largely concentrated on weakly first-order quantum phase transitions (QPT), e.g., the ferromagnetic (FM) transition in MnSi ,^{3,4} the metamagnetic transition in $\text{Sr}_3\text{Ru}_2\text{O}_7$,⁵ and the valence transition in $\text{CeCu}_2(\text{Si}_{1-x}\text{Ge}_x)_2$.⁶

The HF compound YbRh_2Si_2 undergoes an AFM transition at $T_N = 70$ mK.⁷ A small magnetic field or a slight expansion of the unit cell by substituting Si with Ge can eventually suppress the AFM order at a QCP,^{2,8} at which the conventional Landau Fermi-liquid (LFL) theory breaks down (see the inset of Fig. 1). As tuning away from the QCP, LFL behavior immediately recovers at the lowest temperature. On the other hand, the weak AFM transition in YbRh_2Si_2 is stabilized by applying pressure.^{7,9,10} In particular, the magnetic phase undergoes a first-order transition from a small-moment state (AFM-type) to a large-moment state around 10 GPa.⁹ Furthermore, it was argued that in YbRh_2Si_2 FM quantum critical fluctuations dominate over a wide range in the phase diagram except for the close vicinity of the AFM QCP,^{11,12} which seems to be describable in a two impurity Anderson model combined with dynamic mean field theory.¹³ In order to better understand the nature of the “local” QCP, YbIr_2Si_2 , a sister compound of YbRh_2Si_2 , was recently synthesized by Hossain *et al.*¹⁴ YbIr_2Si_2 (I-type) is a moderate HF compound with a paramagnetic ground state at zero pressure and, therefore, was expected to cross a magnetic QCP by applying a small pressure of 2–3 GPa to compress the unit cell volume of YbIr_2Si_2 to that of YbRh_2Si_2 at $p = 0$.¹⁴

In this Brief Report, we present the first high-pressure study for YbIr_2Si_2 . Surprisingly, YbIr_2Si_2 exhibits properties

distinct from YbRh_2Si_2 and shows no evidence for the existence of an AFM QCP at low pressures (see Fig. 1). However, a similar (likely ferro-) magnetic transition is found at high pressures ($p > p_c \approx 8$ GPa). LFL behavior, characterized by $\Delta\rho \sim T^2$, survives in the lowest temperature region. These findings are consistent with the nearly ferromagnetic Fermi-liquid (NFFL) model⁴ and suggest that a first-order FM QPT likely exists in the pressurized Yb compounds. Furthermore, evidence of a pressure-induced valence transition is revealed in YbIr_2Si_2 .

High quality single crystals of YbIr_2Si_2 have been grown from In flux in closed Ta crucibles.¹⁴ Depending on the synthesis conditions, YbIr_2Si_2 can crystallize either in the I-type ThCr_2Si_2 (I4/mmm) as in YbRh_2Si_2 or in the P-type CaBe_2Ge_2 (P4/nmm) structure. The P-type YbIr_2Si_2 is magnetically ordered below 0.7 K, whereas the I-type is a paramagnet.¹⁴ Here we investigate the properties of the I-type YbIr_2Si_2 . High sensitivity, AC four-point measure-

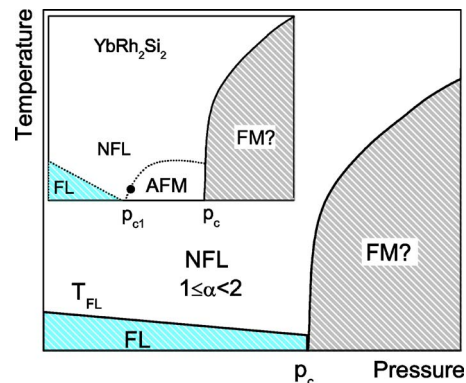


FIG. 1. (Color online) Schematic phase diagram for the Yb compounds other than YbRh_2Si_2 . A large-moment order, presumably FM-type, develops at a critical pressure p_c . The ground-state properties in both the high- p phase and the paramagnetic state can be described by LFL theory. Uniquely, in YbRh_2Si_2 (see the inset, the dot marks its location at $p=0$) AFM phase with weak magnetic moments exists below p_c and vanishes at a QCP (p_{c1}) where the LFL theory is violated.

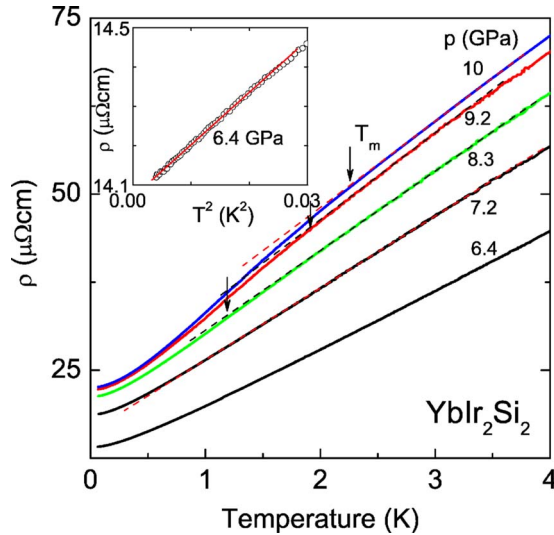


FIG. 2. (Color online) The electrical resistivity $\rho(T)$ ($I||ab$) for YbIr_2Si_2 at various pressures. The downward curvature in $\rho(T)$ as marked by the arrows at T_m indicates the occurrence of a magnetic transition above 8.3 GPa. Inset: The resistivity $\rho(T)$ plotted as a function of T^2 at $p=6.4$ GPa.

ments of the electrical resistivity under high pressure were carried out in a miniature Bridgman cell ($p \leq 10$ GPa) and a piston-cylinder cell ($p < 3$ GPa), filled with either steatite (the former) or fluorinert (the latter) as pressure medium.¹⁵ The pressure is determined from the superconducting transition temperature of Pb (or Sn) mounted inside the cell together with the samples. The experiments were carried out in a Physical Property Measurement System (Quantum Design, down to 1.8 K), a home-made adiabatic demagnetization cooler (~ 250 mK) and a commercial dilution refrigerator (~ 50 mK).

Figure 2 shows $\rho(T)$ ($I||ab$) of YbIr_2Si_2 at various pressures. At $p=0$, the residual resistivity ρ_0 of this sample is about $5 \mu\Omega \text{ cm}$ [residual resistivity ratio (RRR) ≈ 35]. At $p < 8$ GPa, YbIr_2Si_2 is a paramagnet showing a LFL ground state with $\Delta\rho(T) = \rho(T) - \rho_0 = AT^2$ at $T \leq T_{\text{FL}}$ ($T_{\text{FL}} = 150 \sim 200$ mK) (see inset). With increasing temperature, the resistivity deviates from LFL behavior, following $\Delta\rho(T) \sim T^\alpha$ with $\alpha \sim 1$. It is noted that no evidence of magnetism and superconductivity has been detected down to 50 mK even in highly pure samples ($\rho_0 \sim 0.3 \mu\Omega \text{ cm}$, RRR ≈ 350) measured in a hydrostatic piston-cylinder cell. For $p > 8$ GPa, a weak kink at T_m as marked by the arrows in Fig. 2 is observed in the resistivity $\rho(T)$, which becomes more pronounced with increasing pressure. This transition closely resembles the magnetic transitions as found in other Yb compounds,^{7,9,10,16} suggesting a magnetic nature of the transition at T_m . In this context, T_m is determined as the temperature below which $\rho(T)$ shows a downward deviation from the T -linear resistivity as indicated by the dashed lines in Fig. 2.

In Fig. 3(a), the derived values for T_m and T_{FL} are plotted as a function of pressure for YbIr_2Si_2 . Also included in the figure is the value of T_{max} at which $\rho(T)$ reaches a maximum attributed to the onset of coherent Kondo scattering. The value of T_{max} usually scales with the Kondo temperature T_K .

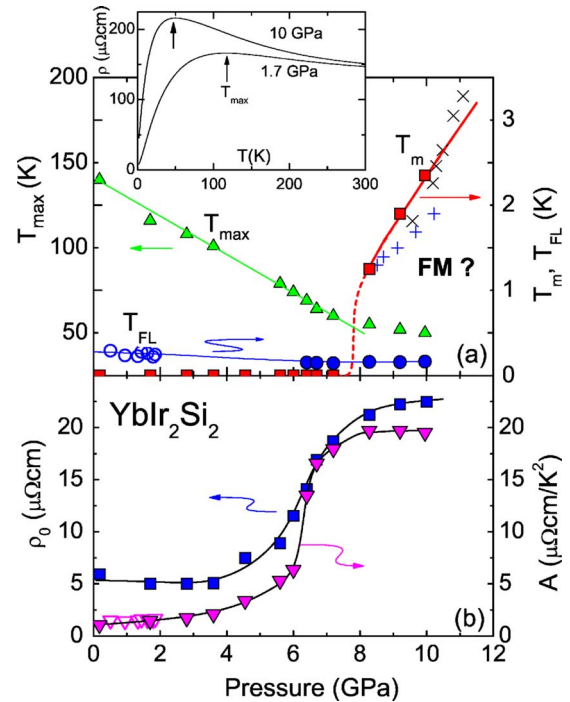


FIG. 3. (Color online) Pressure dependence of (a) T_m , T_{FL} , and T_{max} and (b) the residual resistivity ρ_0 and the resistivity coefficient A for YbIr_2Si_2 . The lines are used as guidance for the eyes. The inset plots $\rho(T)$ over the whole temperature range for $p=1.7$ GPa and 10 GPa. $T_m(p)$ of YbRh_2Si_2 (\times , the high- p phase, from Ref. 10) and of YbCu_2Si_2 ($+$, from Ref. 16) are included for comparison. The open symbols represent data from the sample with RRR ≈ 350 obtained in a clamped cell and the filled symbols are for a sample with RRR ≈ 35 measured in a Bridgman cell. No significant difference can be seen in either T_{FL} or A for these two samples.

In contrast to the Ce-based HF systems, T_{max} of YbIr_2Si_2 monotonically decreases with increasing pressure ($dT_{\text{max}}/dp = -11.3$ K/GPa), becoming saturated at $p_c \approx 8$ GPa above which a magnetic transition appears. Similar features of $T_{\text{max}}(p)$ were observed also in YbCu_2Si_2 ,¹⁶ but not in YbRh_2Si_2 (Refs. 7 and 9) and YbNi_2Ge_2 .¹⁷ In the latter two compounds, the resistivity maximum at T_{max} is split into two maxima under pressure, corresponding to the contributions from the Kondo effect and the crystalline-electric-field (CEF) as frequently observed in the Ce-based HF compounds.

For comparison, the magnetic transitions $T_m(p)$ of YbRh_2Si_2 (the high-pressure phase only)⁹ and YbCu_2Si_2 (Ref. 16) are included in Fig. 3(a). In all these compounds, a magnetic transition appears to abruptly develop above a certain critical pressure ($p_c \sim 8$ GPa), showing a uniform magnetic phase diagram and suggesting a first-order QPT at p_c . Note that one cannot completely exclude the possibility that the weak magnetic transition is smeared out by the enhanced residual scattering while approaching p_c . The magnetic properties of these different Yb compounds appear to be rather similar at sufficiently high pressures, and one may speculate about the nature of the magnetic transition at T_m from the following experimental facts: (i) In both YbIr_2Si_2 (Ref. 14) and YbRh_2Si_2 ,¹² the Sommerfeld-Wilson ratio is strongly en-

hanced compared to other HF systems, indicating that these Yb compounds are close to a FM instability. (ii) The NMR results demonstrated that AFM fluctuations compete with FM fluctuations in YbRh_2Si_2 .¹¹ Upon applying pressure, FM fluctuations may dominate and, therefore, favor a FM-type magnetic structure. (iii) In YbRh_2Si_2 , the ^{170}Yb -Mössbauer effect measurement suggests that the large magnetic moments in the high-pressure phase are aligned along the c axis.⁹ All these features indicate that the pressure-induced transition at T_m is likely of FM nature even though other possibilities cannot be totally excluded at this moment. Further experiments, e.g., neutron scattering, are required to confirm its true nature.

In the NFFL model,^{4,18,19} it is predicted that the conventional LFL behavior survives well below a crossover temperature T^* in both the paramagnetic state and the FM state. Above T^* , the NFFL model reduces to a marginal Fermi-liquid model which allows one to explain the non-Fermi-liquid (NFL) behavior observed at $T > T_{\text{FL}}$. T^* usually vanishes as a magnetic QCP is approached: T^* is inversely proportional to the magnetic correlation length ξ which becomes divergent at a QCP. However, in the case of a first-order magnetic transition near p_c , T^* will be finite.⁴ The experimentally observed FL behavior in the pressurized YbIr_2Si_2 is in fact consistent with the NFFL model, further supporting a FM-type transition at T_m .

Figure 3(b) shows, for YbIr_2Si_2 , the pressure dependence of ρ_0 and the resistivity coefficient A . One notes that the base temperature for data collected in the Bridgman cell is down to 250 mK for $p \leq 6$ GPa and 50 mK for $p > 6$ GPa. The fit of $\Delta\rho = AT^2$ over $0.25 \text{ K} \leq T \leq 0.5 \text{ K}$ can give a reasonable estimation to the coefficient A for $p \leq 6$ GPa, as evidenced by the good agreement with data at lower temperatures measured either in the piston-cylinder cell ($p < 2$ GPa) or in the Bridgman cell at higher pressures ($p > 6$ GPa). An important feature here is the steep increase of both ρ_0 and A setting in, upon increasing pressure, around 6 GPa. Similar phenomena were also observed in YbCu_2Si_2 (Ref. 16) and MnSi ,³ the latter of which was regarded as a typical example to study the FM QPT. Since the characters of the quasiparticles, e.g., the FL ground state with a nearly pressure-independent T_{FL} , appears to be hardly affected while crossing p_c , it is unlikely that here the enhancement of both ρ_0 and A is mainly due to spin fluctuations as usually discussed for systems at a magnetic QCP. Note that T_{FL} dramatically increases as tuning away from the QCP in MnSi .⁴ Alternatively, the occurrence of these unique features in YbIr_2Si_2 might be related to a valence change as discussed below.

In most cases, intermediate-valence compounds have a much lower Kadowaki-Woods (KW) ratio A/γ^2 ($\sim 0.4 \mu\Omega \text{ cm mol}^2 \text{ K}^2 \text{ J}^{-2}$) than the HF compounds ($10 \mu\Omega \text{ cm mol}^2 \text{ K}^2 \text{ J}^{-2}$) due to the full degeneracy of the ground state.²⁰ In YbIr_2Si_2 and YbCu_2Si_2 , the CEF splitting Δ_{CEF} can be comparable to the Kondo temperature, leading to a moderate value of the KW ratio: $A/\gamma^2 = 2-5 \mu\Omega \text{ cm mol}^2 \text{ K}^2 \text{ J}^{-2}$. Upon applying pressure, T_K is reduced and the ground state could be strongly affected by the CEF effect. As a result, the KW ratio can be enhanced due to the reduction of the f -orbital degeneracy. Since $T_{\text{max}} \sim T_K \sim \gamma^{-1}$, the value of A/γ^2 can be measured by AT_{max}^2 . In Fig.

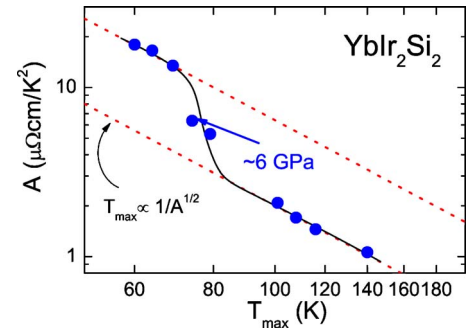


FIG. 4. (Color online) The log-log plot of the coefficient A and T_{max} (with p as an implicit parameter), showing that $AT_{\text{max}}^2 = \text{const}$ with distinct constants for $p > 6$ GPa and $p < 6$ GPa, respectively.

4, we plot A vs T_{max} in a log-log plot, in which the dashed lines follow $A \sim T_{\text{max}}^{-2}$. One can see that a transition takes place around $p = 6$ GPa, on either side of which AT_{max}^2 is a constant, but with different values. For $6 \text{ GPa} < p < 8 \text{ GPa}$, a large value of KW ratio ($A/\gamma^2 \sim 20 \mu\Omega \text{ cm mol}^2 \text{ K}^2 \text{ J}^{-2}$) is derived from the scaling of AT_{max}^2 . The decrease of A/γ^2 around 6 GPa indicates a weak valence transition attributed to the change of f -orbital degeneracy. This assertion is further supported by the resistivity isotherms $\Delta\rho(T, p) = \rho(T, p) - \rho_0(p)$ as shown in Fig. 5. The large decrease of $\Delta\rho(T, p)$ (at low- T) and A below $p = 6.4$ GPa implies a weakening of electronic correlations as a result of the delocalization of f electrons at lower pressures.

Similar features of $\Delta\rho(T, p)$, ρ_0 , and the coefficient A as demonstrated in YbIr_2Si_2 were previously found in $\text{CeCu}_2(\text{Si}_{1-x}\text{Ge}_x)_2$ at a weak first-order volume-collapse transition.⁶ Indeed, a theoretical model based on valence fluctuations predicts a pronounced enhancement of ρ_0 and A as well as the T -linear resistivity above a crossover temperature T_v at a valence transition,²¹ consistent with our findings here. How these two (magnetic and valence) transitions are interacting with each other remains an interesting question which cannot, however, be answered based on the available results. For example, in YbCu_2Si_2 the magnetic transition appears around 8 GPa, but ρ_0 and A peak at 10 GPa, where the KW relation starts to deviate.¹⁶ On the other hand, in

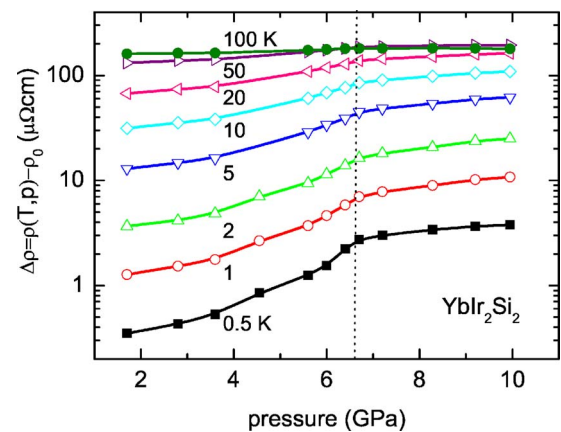


FIG. 5. (Color online) Pressure dependence of the resistivity isotherms $\Delta\rho(p) [= \rho(T, p) - \rho_0(p)]$ at various temperatures.

YbIr₂Si₂ the valence transition appears prior to the magnetic transition. Interestingly, the valence transition seems to be accompanied by a strong enhancement of ρ_0 and A .

The cause for the unique appearance of the low-pressure AFM phase in YbRh₂Si₂ (Refs. 7, 9, and 10) [and possibly also in YbNi₂Ge₂ (Ref. 17)] remains unclear. One possibility might be related to the band structure, e.g., the distinct values of the density of state (DOS) at the Fermi energy $N(E_F)$, originating from the different electronic configurations of Rh and Ir. While the intrasite coupling constant J between f and conduction electrons may experience similar modulation under pressure, the value of $N(E_F)J$ may vary from compound to compound because of the different values of $N(E_F)$. In YbRh₂Si₂, $N(E_F)$ can be small because the DOS peaks just below E_F .²² The resulting small value of $N(E_F)J$ then may favor magnetic ordering even at low pressures, while in YbIr₂Si₂ and YbCu₂Si₂ the Kondo effect may dominate in the same pressure region, leading to a nonmagnetic ground state.²³ These arguments are compatible with the pressure dependence of T_{\max} . T_{\max} reaches a few kelvins in YbRh₂Si₂

(Ref. 9) and YbNi₂Ge₂,¹⁷ but 50 K in YbIr₂Si₂ and YbCu₂Si₂ (Ref. 16) at p_c , indicating a predominant Ruderman-Kittel-Kasuya-Yosida (RKKY) interaction in YbRh₂Si₂. The intersite RKKY coupling can change sign and, therefore, give rise to a different type of magnetic ordering under pressure.

In summary, we have shown that a FM-type quantum phase transition is likely to exist in the Yb compounds under sufficiently high pressure and that the related properties may be well described within the NFFL model. These findings will be essentially important for understanding the unusual properties of YbRh₂Si₂, especially its complex p - T phase diagram, and will stimulate further exploration of FM quantum criticality in the HF systems. Moreover, a weak valence transition accompanied by a huge enhancement of ρ_0 and the resistivity coefficient A appears to exist in these pressurized Yb systems. To elucidate these remarkable properties, further experimental and theoretical efforts are highly desired.

We thank Q. Si and M. B. Salamon for stimulating discussions. H.Q.Y. acknowledges the ICAM.

*Electronic address: yuan@mrl.uiuc.edu

- ¹See, e.g., P. Thalmeier, G. Zwirgagl, O. Stockert, G. Sparn, and F. Steglich, in *Frontiers in Superconducting Materials*, edited by A. V. Narlikar (Springer-Verlag, Berlin, 2005), p. 109.
- ²J. Custers, P. Gegenwart, H. Wilhelm, K. Neumaier, Y. Tokiwa, O. Trovarelli, C. Geibel, F. Steglich, C. Pepin, and P. Coleman, *Nature (London)* **424**, 524 (2003).
- ³C. Thessieu, J. Flouquet, G. Lapertot, A. N. Stepanov, and D. Jaccard, *Solid State Commun.* **95**, 707 (1995).
- ⁴C. Pfleiderer, G. J. McMullan, S. R. Julian, and G. G. Lonzarich, *Phys. Rev. B* **55**, 8330 (1997); N. Doiron-Leyraud, I. R. Walker, L. Taillefer, M. J. Steiner, S. R. Julian, and G. G. Lonzarich, *Nature (London)* **425**, 595 (2003).
- ⁵S. A. Grigera, R. S. Perry, A. J. Schofield, M. Chiao, S. R. Julian, G. G. Lonzarich, S. I. Ikeda, Y. Maeno, A. J. Millis, and A. P. Mackenzie, *Science* **294**, 329 (2001); S. A. Grigera, P. Gegenwart, R. A. Borzi, F. Weickert, A. J. Schofield, R. S. Perry, T. Tayama, T. Sakakibara, Y. Maeno, A. G. Green, and A. P. Mackenzie, *ibid.* **306**, 1154 (2004); P. Gegenwart, F. Weickert, M. Garst, R. S. Perry, and Y. Maeno, *Phys. Rev. Lett.* **96**, 136402 (2006).
- ⁶H. Q. Yuan, F. M. Grosche, M. Deppe, C. Geibel, G. Sparn, and F. Steglich, *Science* **302**, 2104 (2003); H. Q. Yuan, F. M. Grosche, M. Deppe, G. Sparn, C. Geibel, and F. Steglich, *Phys. Rev. Lett.* **96**, 047008 (2006).
- ⁷O. Trovarelli, C. Geibel, S. Mederle, C. Langhammer, F. M. Grosche, P. Gegenwart, M. Lang, G. Sparn, and F. Steglich, *Phys. Rev. Lett.* **85**, 626 (2000).
- ⁸P. Gegenwart, J. Custers, C. Geibel, K. Neumaier, T. Tayama, K. Tenya, O. Trovarelli, and F. Steglich, *Phys. Rev. Lett.* **89**, 056402 (2002).
- ⁹J. Plessel, M. M. Abd-Elmeguid, J. P. Sanchez, G. Knebel, C. Geibel, O. Trovarelli, and F. Steglich, *Phys. Rev. B* **67**, 180403(R) (2003).
- ¹⁰G. Knebel, V. Glazkov, A. Pourret, P. G. Niklowitz, G. Lapertot, B. Salce, and J. Flouquet, *Physica B* **359–361**, 20 (2005).
- ¹¹K. Ishida, K. Okamoto, Y. Kawasaki, Y. Kitaoka, O. Trovarelli, C. Geibel, and F. Steglich, *Phys. Rev. Lett.* **89**, 107202 (2002).
- ¹²P. Gegenwart, J. Custers, Y. Tokiwa, C. Geibel, and F. Steglich, *Phys. Rev. Lett.* **94**, 076402 (2005).
- ¹³P. Sun and G. Kotliar, *Phys. Rev. Lett.* **95**, 016402 (2005).
- ¹⁴Z. Hossain, C. Geibel, F. Weickert, T. Radu, Y. Tokiwa, H. Jeevan, P. Gegenwart, and F. Steglich, *Phys. Rev. B* **72**, 094411 (2005).
- ¹⁵H. Q. Yuan, Ph.D. thesis, Technische Universität Dresden, 2003.
- ¹⁶K. Alami-Yadri, H. Wilhelm, and D. Jaccard, *Eur. Phys. J. B* **6**, 5 (1998); H. Winkelmann, M. M. Abd-Elmeguid, H. Micklitz, J. P. Sanchez, P. Vulliet, K. Alami-Yadri, and D. Jaccard, *Phys. Rev. B* **60**, 3324 (1999).
- ¹⁷G. Knebel, D. Braithwaite, G. Lapertot, P. C. Canfield, and J. Flouquet, *J. Phys.: Condens. Matter* **13**, 10935 (2001).
- ¹⁸T. Moriya, *Spin Fluctuations in Itinerant Electron Magnetism* (Springer, Berlin, 1985).
- ¹⁹J. A. Hertz, *Phys. Rev. B* **14**, 1165 (1976); A. J. Millis, *ibid.* **48**, 7183 (1993).
- ²⁰N. Tsujii, H. Kontani, and K. Yoshimura, *Phys. Rev. Lett.* **94**, 057201 (2005).
- ²¹K. Miyake and H. Maebashi, *J. Phys. Soc. Jpn.* **71**, 1007 (2002); A. T. Holmes, D. Jaccard, and K. Miyake, *Phys. Rev. B* **69**, 024508 (2004).
- ²²T. Jeong and W. E. Pickett, *J. Phys.: Condens. Matter* **18**, 6289 (2006).
- ²³S. Doniach, *Physica B & C* **91**, 231 (1977).